Deep view of the HESS J1303-631 region with *Fermi*-LAT: an SNR in disguise?

•••

Martín Moró González,

Iurii Sushch, Marine Pihet, Emma de Oña Willhelmi, Igor Oya Vallejo, Christopher Burger-Scheidlin and Miroslav Filipović

Centro de Investigaciones Energéticas, Medioambientales y Tecnológicas (CIEMAT),
Universidad Autónoma de Madrid (UAM)

TeV Particle Astrophysics 2026, Tendō, Japan

HESS J1303-631

- Detected in 2005 [1].

- Nearest detected sources:
  - Supernova Remnant (SNR) Kes-17 (G304.6+0.1).
  - Binary system PSR B1259-63.

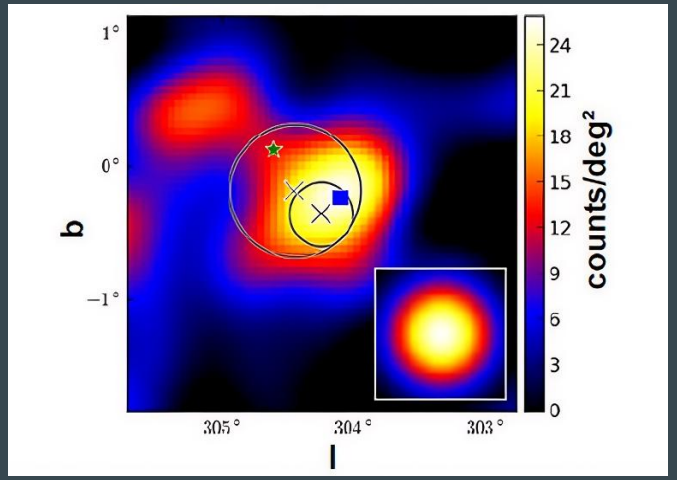

Counts map of 45 months of *Fermi*-LAT data. [2]

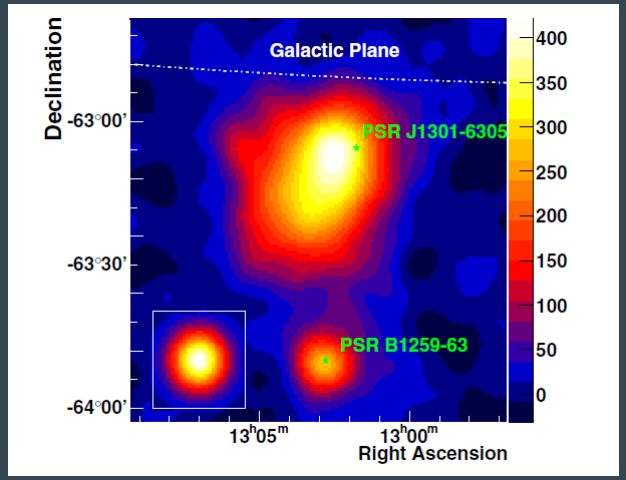

H.E.S.S. Collaboration 2012.

[1]: Aharonian, F. et al. 2005
[2]: F. Acero et al 2013

PWN association

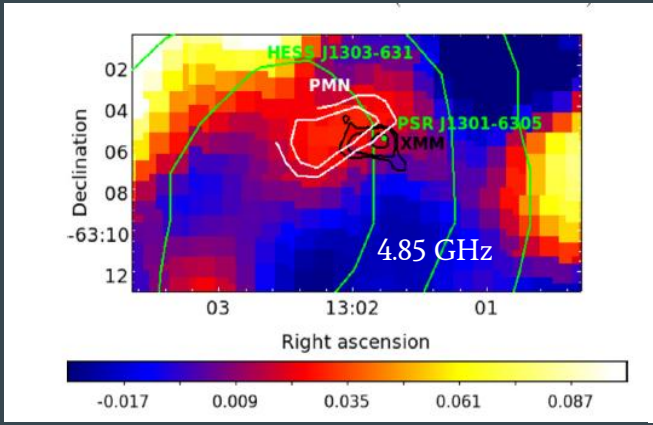

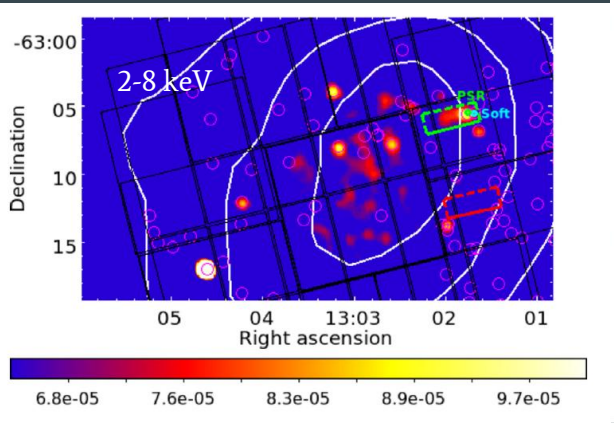

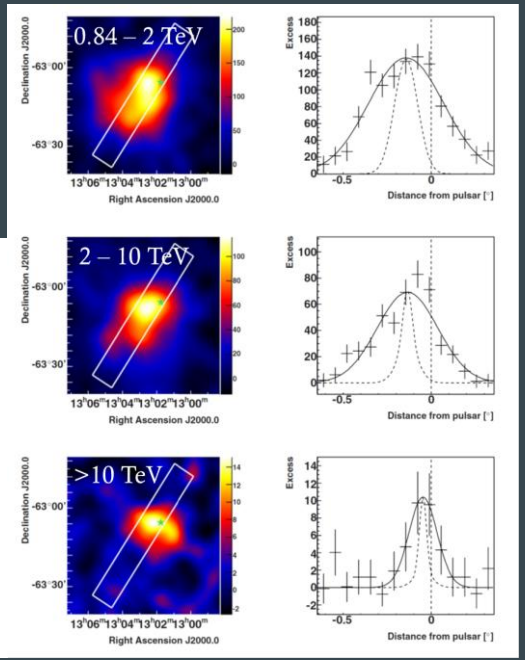

4.85 GHz radio image from the PMN survey

XMM-Newton X-ray flux map at 2-8 keV

Excess map in different TeV energy bands.

H.E.S.S. Collaboration, et al. 2012

Radio observations (ATCA)

- Radio observations at 1.384 GHz of the vicinity did not show any counterpart of the PWN [3].

- However, a shell-like structure was revealed.

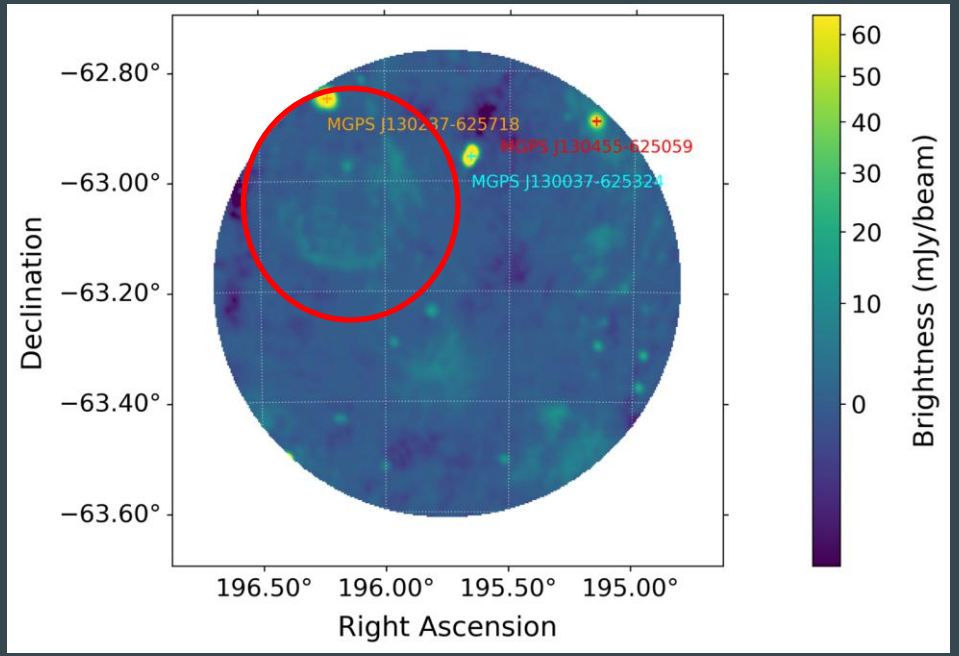

ATCA observation of HESS J1303-631.

[3]: Sushch, I. et al. 2017

Radio observations (ATCA)

- Radio observations at 1.384 GHz of the vicinity did not show any counterpart of the PWN [3].
- However, a shell-like structure was revealed.
- Currently an SNR candidate (G3404.4-0.2), named Mavka.

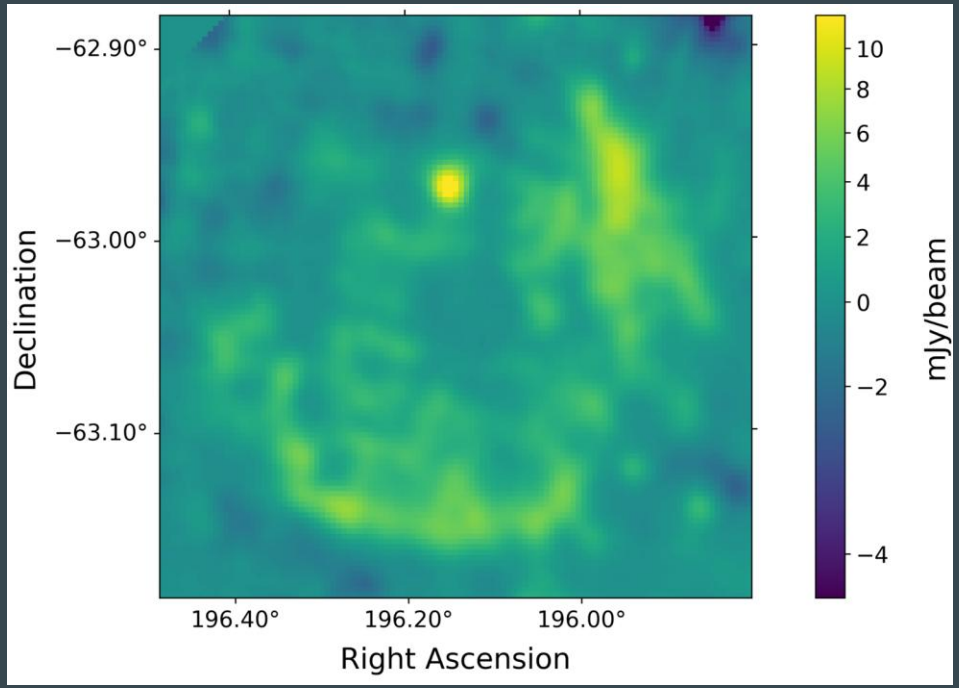

SNR candidate G3404.0-0.2.

Radio observations

- Radio observations at 1.384 GHz of the vicinity did not show any counterpart of the PWN.
- However, a shell-like structure was revealed.
- ASKAP and MeerKAT surveys supported the observation [4,5].

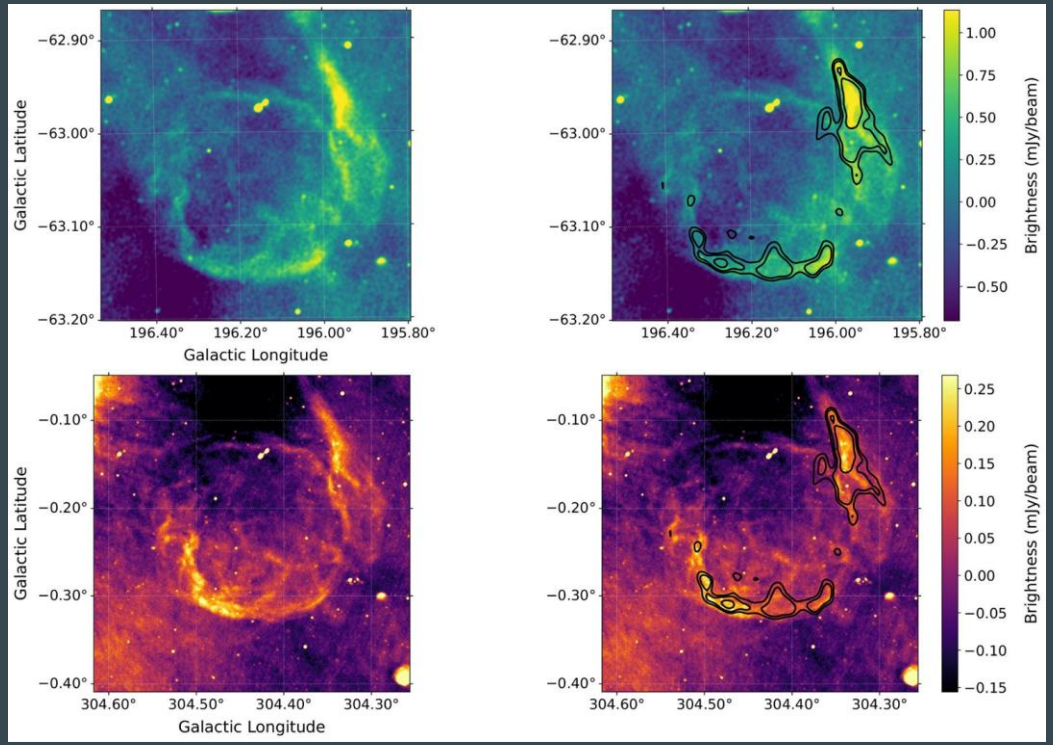

Top (Bottom): Mavka detection in ASKAP(MeerKAT) galactic plane survey [4, 5].

[4]: Anderson, L. D. et al. 2025
[5]: Ball, B. D. et al. 2025

Increase in dataset of *Fermi*-LAT data

45 months of data.

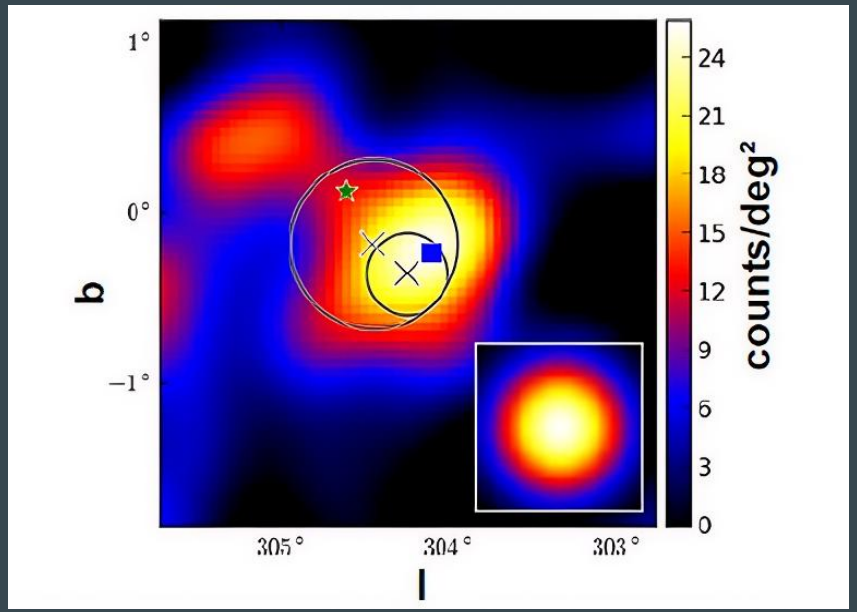

17 years of data

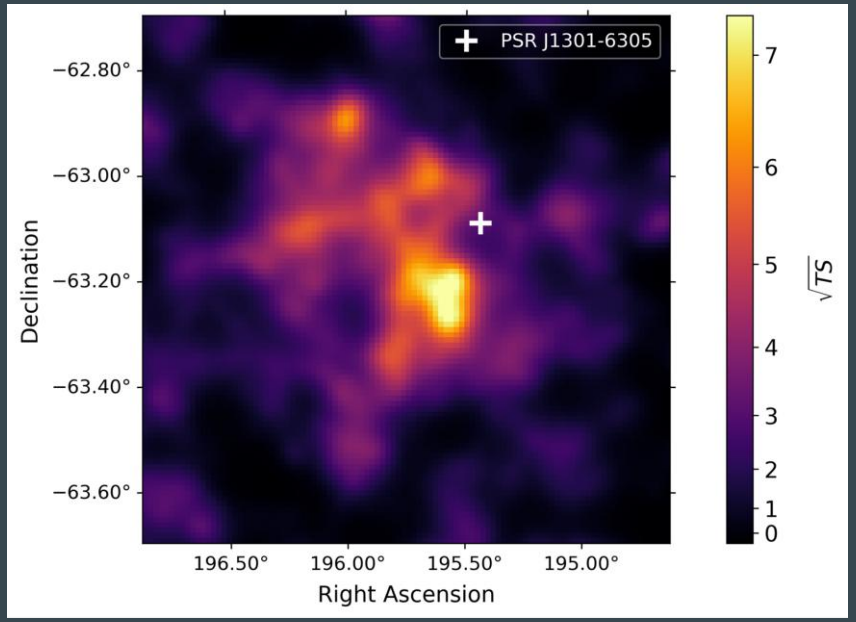

Fermi-LAT analysis

- The current modeling of HESS J1303-631 in the *Fermi*-LAT Fourth Source Catalog (4FGL) presents the PWN as a symmetric Gaussian with radius 0.24º.

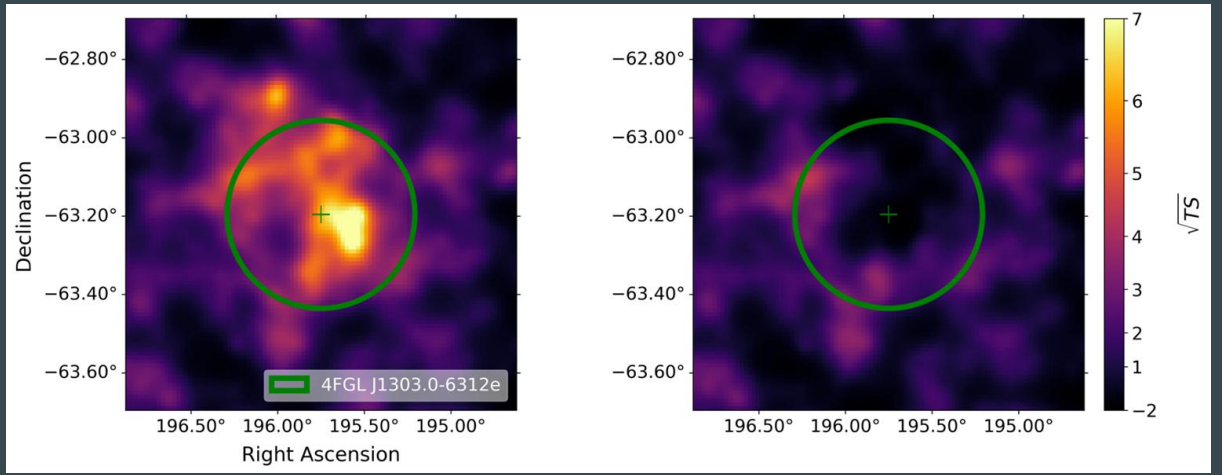

Left: map of 4FGL J1303.0-6312e before modeling. Right: map after including it as a model component. Green circle(cross) presents the extension(centre) of the Gaussian.

Fermi-LAT analysis

- The current modeling of HESS J1303-631 in the *Fermi*-LAT Fourth Source Catalog (4FGL) presents the PWN as a symmetric Gaussian with radius 0.24º.
- The addition of Mavka did not yield a significant statistical improvement.

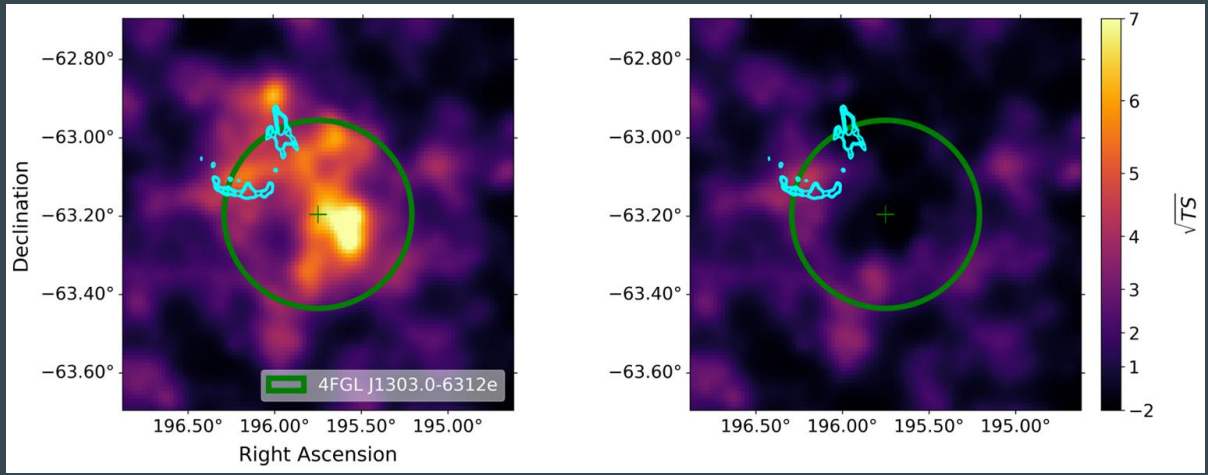

Same as previous maps adding Mavka's spatial position.

Fermi-LAT analysis

- The current modeling of HESS J1303-631 in the *Fermi*-LAT Fourth Source Catalog (4FGL) presents the PWN as a symmetric Gaussian with radius 0.24º.
- The addition of Mavka did not yield a significant statistical improvement.
- Recent analysis have claimed a 68% containment radius of R_{68} = 0º.32 ±0º.04 [6].

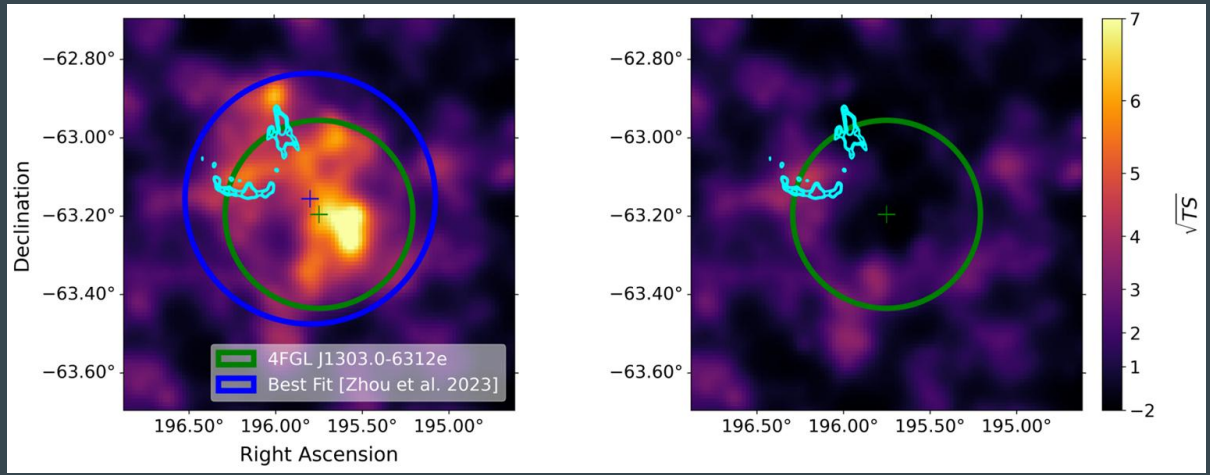

Same as previous maps adding recent analysis. Blue circle(cross) presents the best fit extension(centre) of the Gaussian [6].

[6]: Zhou, L.-C. et al. 2023

Fermi-LAT analysis

- Regarding the emission peaks present in the region, four different peaks with $\sigma > 4.5$ were found.

	TS ($\sigma = \sqrt{TS}$)	Index
Source 1	81.67	1.77 ± 0.3
Source 2	45.03	1.4 ± 0.16
Source 3	24.62	1.75 ± 0.37
Source 4	25.69	1.87 ± 0.29

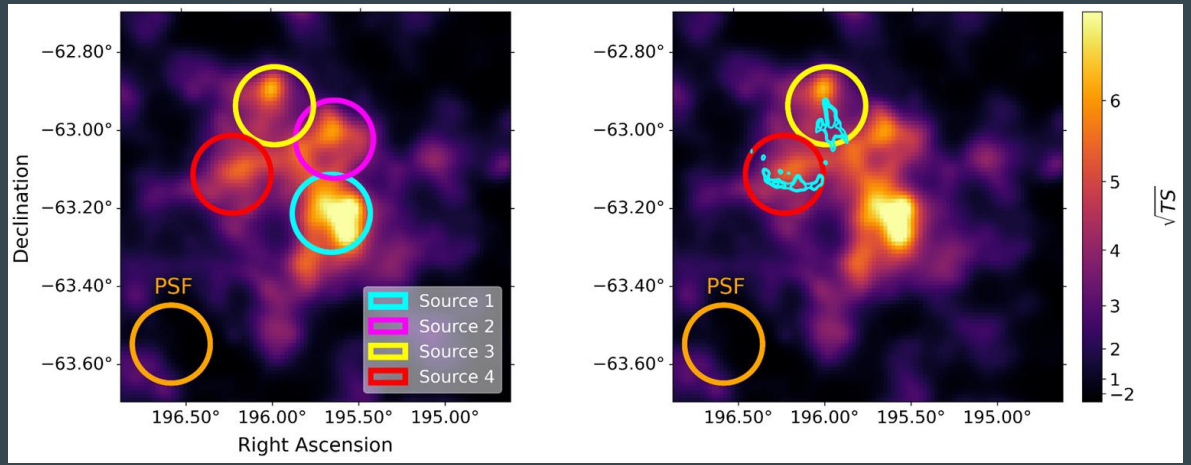

Left: Emission peaks of 4FGL J1303.0-6312e surroundings. Right: coincidence of Mavka with two emission peaks.

Fermi-LAT analysis

- The inclusion of the ATCA template into the analysis yielded a TS = 55.63.

	Index
HESS J1303-631	1.77 ± 0.15
Mavka	1.71 ± 0.14
Mana	1.43 ± 0.17

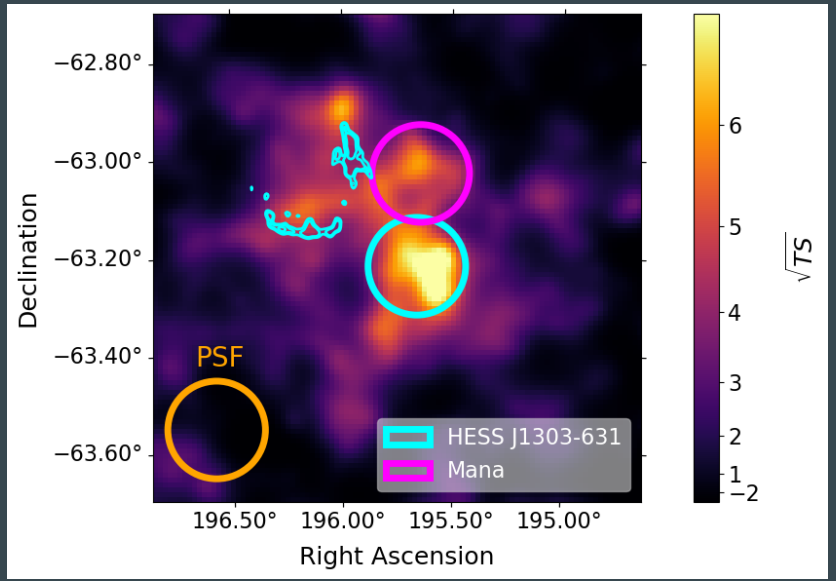

Sources 3 and 4 were replaced with Mavka's template and source 2 was named Mana.

Spectral Energy Distribution (SED)

	Index
HESS J1303-631	1.77 ± 0.15
Mavka	1.71 ± 0.14
Mana	1.43 ± 0.17

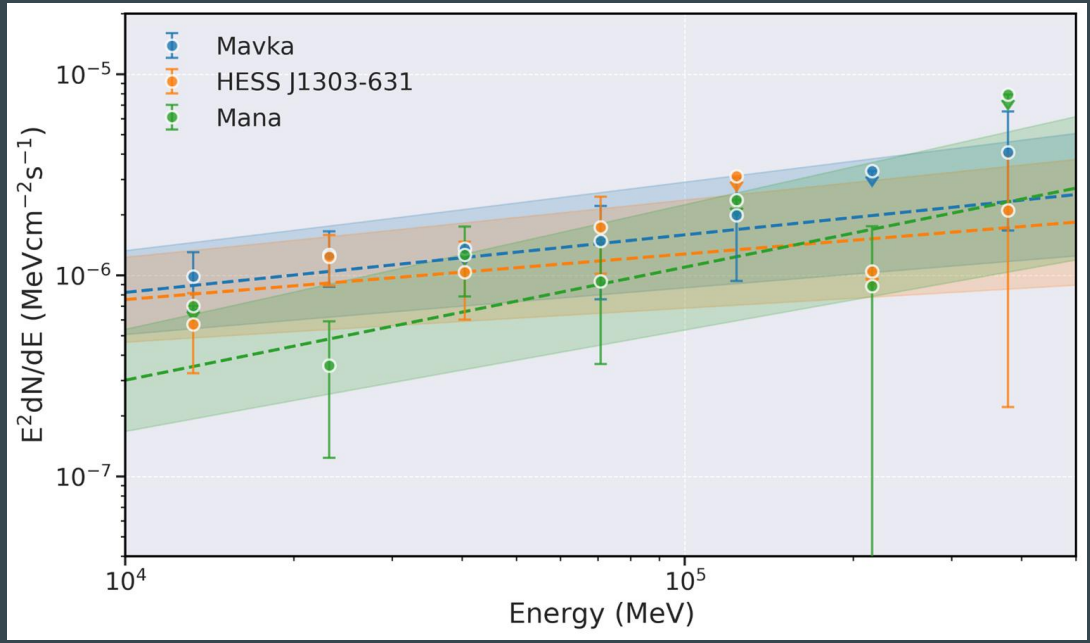

Spectral Energy Distribution (SED) of HESS J1303-631 modelled as a point source, Mavka and Mana.

Data analysis conclusions

- A single symmetric gaussian is still preferred over any proposed modeling.
- Current modeling might underestimate the number of sources present.
- The morphological and spectral analysis combined with multiwavelength data presents the hint of detection of two new sources, Mavka and Mana.

Mavka, the birthplace of pulsar PSR J1301-6305?

- Main arguments:
  - Proximity of Mavka
  - X-ray nebula tail.
- Dispersion Measure (DM) suggests a distance of 4.7 kpc [7] (previouly 6.6 kpc [8]).
- Characteristic age: 11 kyr [9].
- Projected velocity of the pulsar: $2200 - 3100$ km/s (fastest pulsar known).

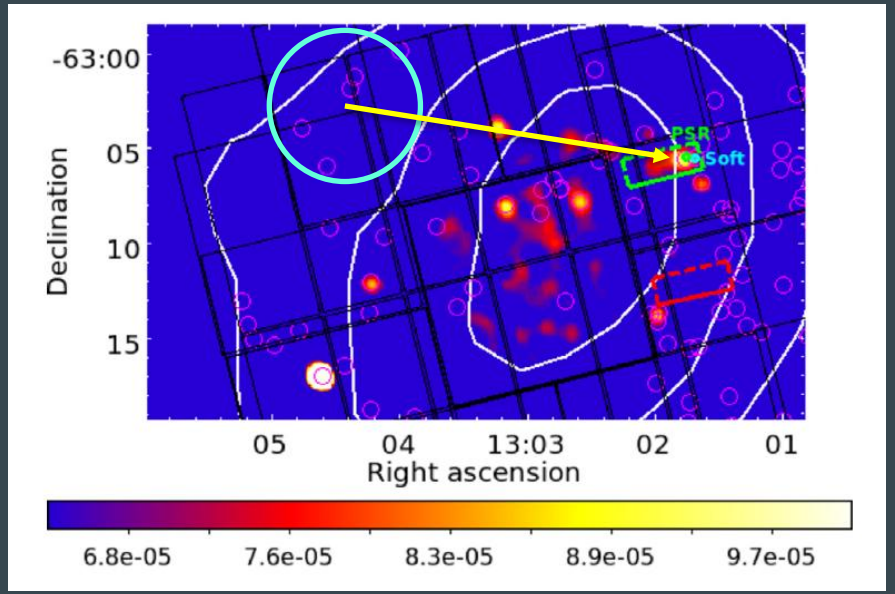

H.E.S.S. Collaboration, et al. 2012

[7]: Ocker, S. K. & Cordes, J. M. 2026
[8]: Cordes, J. M. & Lazio, T. J. W. 2002
[9]: Manchester, R. N et al. 2005

Mavka, the birthplace of pulsar PSR J1301-6305?

- Main arguments:
  - Proximity of Mavka
  - X-ray nebula tail.
- Dispersion Measure (DM) suggests a distance of 4.7 kpc [7] (previouly 6.6 kpc [8]).
- Characteristic age: 11 kyr [9].
- Projected velocity of the pulsar: $2200 - 3100$ km/s (fastest pulsar known).

- The length of the X-ray tail is defined by synchrotron cooling:

$$L = v_p \tau_{cool}(\gamma_{th}, B_{tail})$$

$$v_p = 3052 \left[\frac{d_p}{4.7\ \text{kpc}}\right]\left[\frac{\Delta}{150''}\right]\left[\frac{B_{tail}}{10\ \mu\text{G}}\right]^{\frac{3}{2}}\left[\frac{E_X}{2\ \text{keV}}\right]^{\frac{1}{2}} \text{km/s}$$

- Strongly dependent on the magnetic field in the X-ray tail: $B_{tail} \sim 1 - 2\ \mu$G [6, 10] $\rightarrow v_p \sim 100 - 300$ km/s.

[7]: Ocker, S. K. & Cordes, J. M. 2026
[8]: Cordes, J. M. & Lazio, T. J. W. 2002
[9]: Manchester, R. N et al. 2005
[10]: H.E.S.S. Collaboration, et al. 2012

Non-thermal emission

- Particle distribution:

$$f(E) = A\left(\frac{E}{E_0}\right)^{-\alpha} \exp\left(-\frac{E}{E_{cutoff}}\right)$$

- Assumed distance of 4.7 kpc.

log10(norm)	$35.18\ ^{+0.17}_{-0.13}$
Index	1.83 ± 0.09
E_{cutoff} (TeV)	$4.0\ ^{+2.0}_{-1.4}$
Magnetic field (μG)	$3.9\ ^{+1.7}_{-1.1}$

W_e (erg) x 10^{48}	$2.6\ ^{+1.0}_{-0.7}$

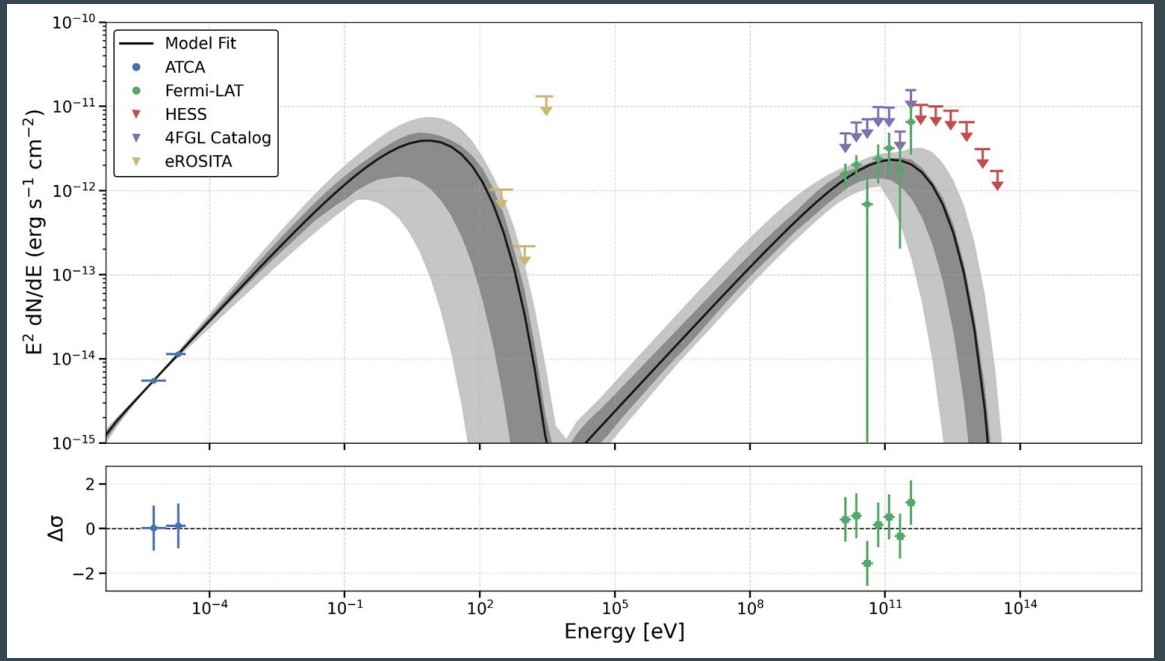

Synchrotron and Inverse Compton emission of Mavka computed with naima.

Multi-source scenario

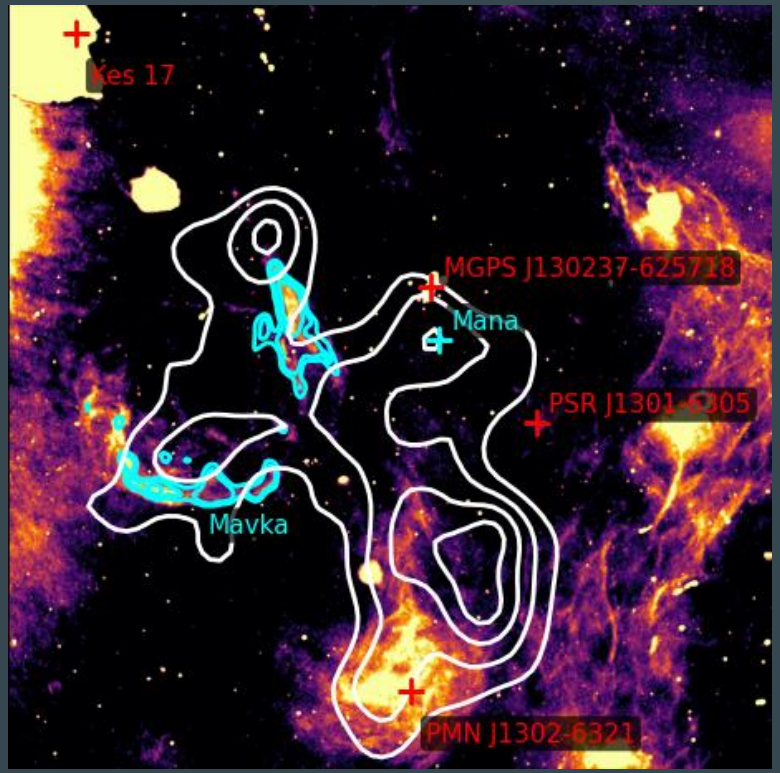

1.38 GHz MeerKAT radio image overlaid with *Fermi*-LAT contours of 4FGL J1303.0-6312e.

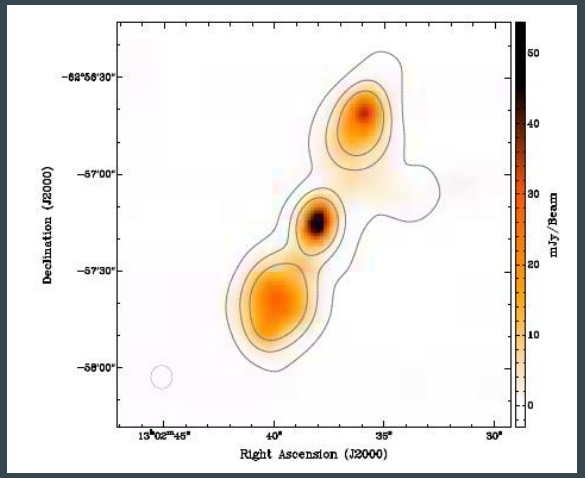

Radio image of MGPSJ130237-625718 at 2.368 GHz [3].

Next steps?

- CTAO simulations were conducted to check whether it will have the capacity to resolve between the two, or three, sources.
- Two different scenarios for Mavka's spectral model:
  - Simple power law.
  - Exponential cutoff power law.

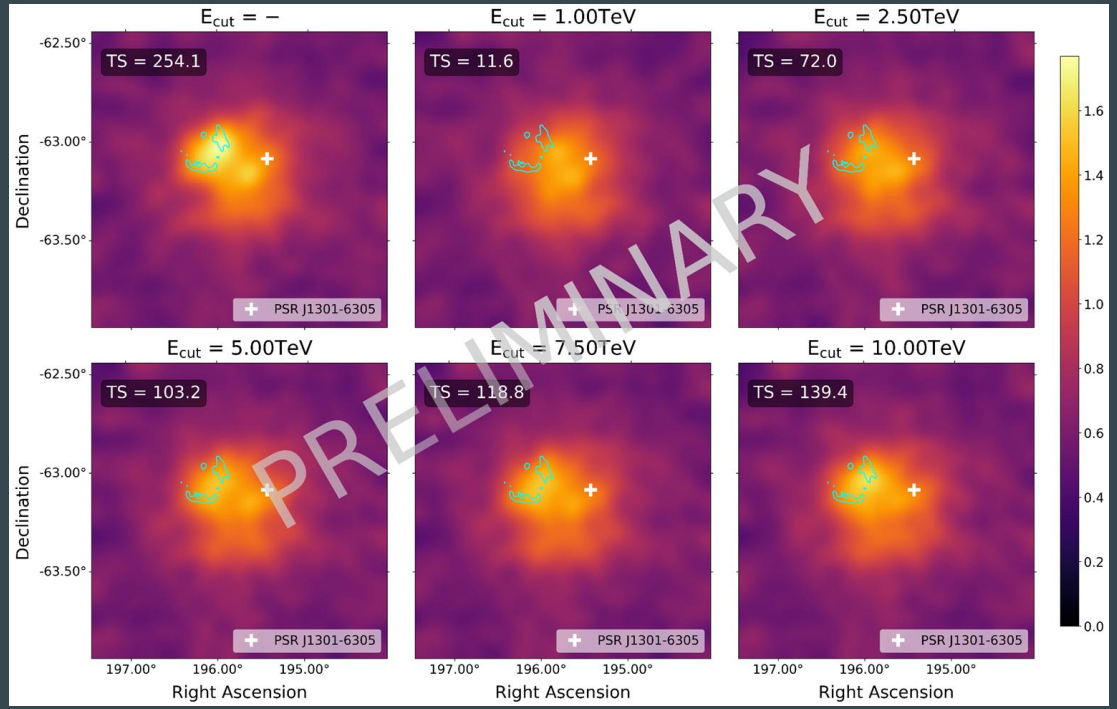

CTAO simulations of HESS J1303-631 and Mavka.

Thanks!

...

Back-up slides

...

Residuals of Mavka in CTAO simulations

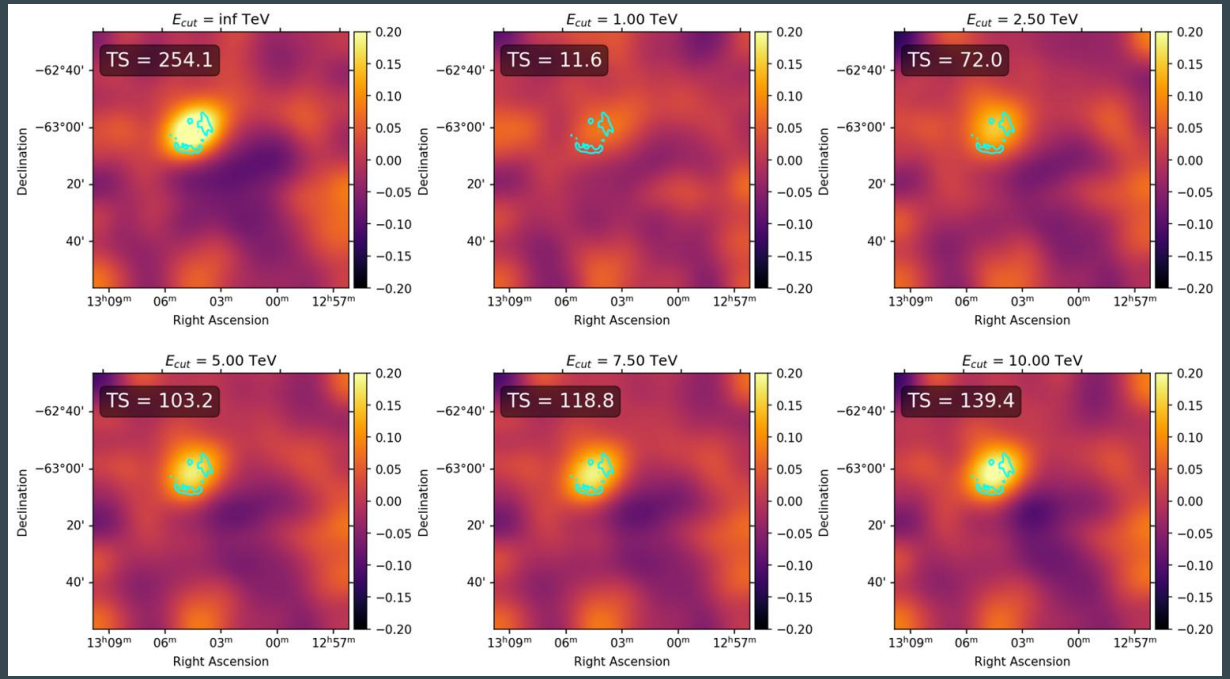

Mavka residuals in CTAO simulations.

Energy-dependent morphology

- For energies < 0.84 TeV, the current modeling in the 4FGL catalog was considered.
- For energies > 0.84 TeV, HESS J1303.631 was modeled as a two-dimensional asymmetric Gaussian function, with major (minor) Gaussian width axis of 0.194º ± 0.08º (0.145º ± 0.06), with a position angle of ϕ = 147º ± 6º, counterclockwise from the north.

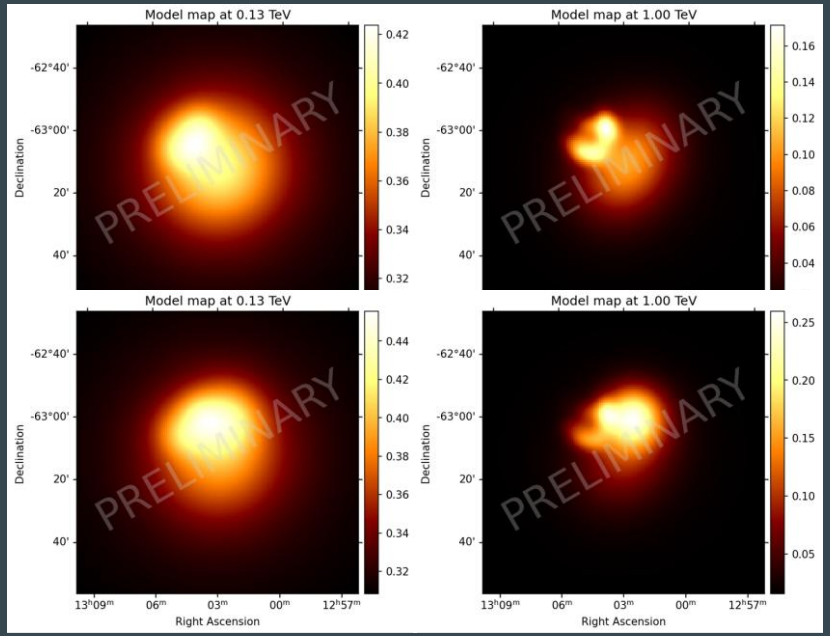

Top: Model map in CTAO simulations with HESS J1303-631 morphology modeled as energy-dependent. Bottom: Same but including Mana's presence.

CTAO simulations including Mana's presence counts map

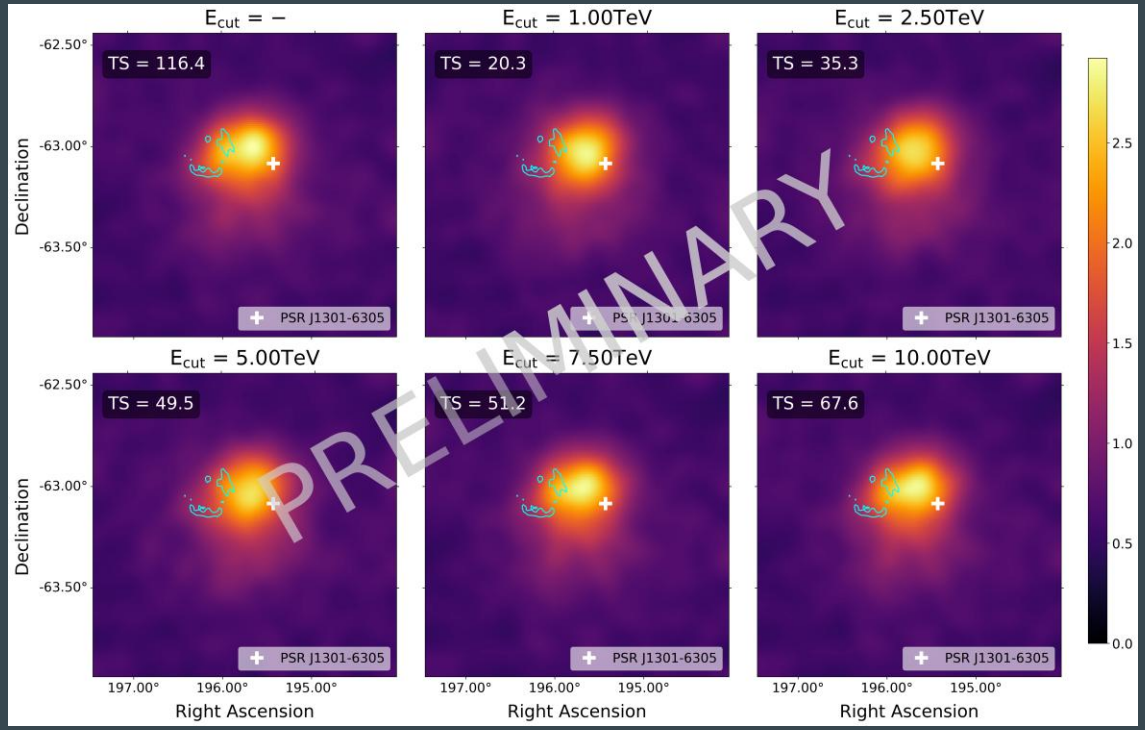

Residuals of Mavka in CTAO simulations including Mana's presence